PHYSICS AND CHEMISTRY OF SOLID STATE
V. 24, No. 4 (2023) pp. 765-773
Section: Physics

DOI: 10.15330/pcss.24.4.765-773

Vasyl Stefanyk Precarpathian National University

ФІЗИКА І ХІМІЯ ТВЕРДОГО ТІЛА
Т. 24, № 4 (2023) С. 765-773
Фізико-математичні науки

PACS: 61.72.Cc, 64.75.Op, 66.30.Dn, 66.30.Ny, 66.30.Pa, 68.35.Fx, 68.35.Rh ISSN 1729-4428

M.V. Yarmolenko[1,2], S.O. Mogilei[1]

Copper and Aluminium Electrochemical Corrosion Investigation during Electrolysis and Heating from 20°C to 180°C by Mathematical Modelling

[1]*Rauf Ablyazov East European University, Cherkasy, Ukraine, yarmolenko@suem.edu.ua*
[2]*Scientific Research Institute of Armament and Military Equipment Testing and Certification, Cherkasy, Ukraine*

Our investigations show that electrochemical corrosion of copper is faster than electrochemical corrosion of aluminium at temperatures below 180°C and electric current density 3,000 A/m^2 (or 30 A/dm^2=3 mA/mm^2). We have obtained that aluminium anodes (cylindrical or spherical) dissolve into concentrated NaCl solution during electrolysis more rapidly with temperature increasing while copper anodes (cylindrical or spherical) dissolve more slowly with temperature increasing from room temperature to temperature 180°C. Electric current value also increases with temperature increasing. Really, such result is unexpected. General quantity of the H^+ and Cl^- ions decreases during electrolysis at all temperatures since the H_2 and Cl_2 gases are formed near electrodes. It decreases electric current value on 1.3%. General quantity of the Cu^+ and Cu^{2+} ions decreases with temperature increasing too. We guess that one reason only should be for electric current value increasing: average charge of copper ions increases from +1 at room temperature to +1.5 at 100°C and to +2 at 180°C while charge of aluminium ions remains the same +3. Corresponding mathematical model is proposed for the analysis, and literature experimental data are used too.

Keywords: electrochemical corrosion, electrolysis, electrocoagulation, copper, aluminium, mathematical modelling, metallic coating.

Received 18 May 2023; Accepted 07 December 2023.

Introduction

Copper (Cu) coatings on an aluminium (Al) wire, that are widely used in the automobile and aerospace industries to reduce of total weight of the electric wires, can be quickly destroyed during working since they are heated up to 200°C [1]. On the other hand, thin Al pad (≈ 1 μm thickness) can prevent gold and copper corrosion, because intermetallics formation rate in the Au-Al system is higher than intermetallics formation rate in the Cu-Al system, so it is possible to use Cu instead of gold (Au) for wire bonding in microelectronics packaging [2]. In addition, the container, which consists of an outer copper canister and an inner carbon steel (Fe) tank, is used to dispose of spent nuclear fuel [3-6]. Otherwise, corrosion of copper (Cu) and its alloys is a problem due to their large-scale use in drinking water pipelines, leading to premature failure of pipes and fittings, increased toxicity due to Cu release and expensive costs associated with Cu removal in wastewater [7, 8]. Moreover, an excess of dissolved copper causes accelerated corrosion in iron pipelines, which are widely used in the water distribution system [9]. Therefore, it is important to compare the corrosion rates of Cu and Al at different temperatures (from 5°C to 180°C) in solutions of salts in water.

Electrochemical corrosion of Cu and Al was investigated at constant temperatures 20°C and 100°C during 5, 10, 15, and 20 min [10-14] and at temperatures T_1 = 175°C, T_2 = 200°C, and T_3 = 225°C during 120, 240, 360, and 480 h (without applied external voltage) [2].

We can find copper containing species in the copper-chlorine-water system at temperatures 5 – 100°C in Table 4 in [3, 4]: CuCl(cr), CuCl(aq), $CuCl_2^-$, $CuCl_3^{2-}$, $Cu_2Cl_4^{2-}$,

$Cu_3Cl_6^{3-}$ for Cu^+ and $CuCl^+$, $CuCl_2(aq)$, $CuCl_3^-$, $CuCl_4^{2-}$, $CuCl_2 3Cu(OH)_2(s)$ for Cu^{2+}.

Diffusion kinetics in solid state are different in planar, cylindrical, and spherical samples [15], so we planned to analyse the electrochemical degradation of cylindrical and spherical copper (Cu) and aluminium (Al) anodes in an electrolyte (concentrated aqueous NaCl solution) under different temperature conditions.

Copper (Cu), iron (Fe), and aluminium (Al) anodes and cathodes are used also for wastewater remediating by electrocoagulation (EC) [16]. The EC process produces ions (Cu^+, Cu^{2+}, Fe^{2+}, Fe^{3+} or Al^{3+}) during electrolysis that capable of producing coagulants in water solutions.

Aluminium undergoes dissolution to the Al^{3+} ions in all types of electrodes at different temperatures [16]. Two aluminium electrodes were used for the removal of cadmium (Cd) from wastewater through the EC process and various EC tests were conducted for the different initial temperatures of 18, 30, 50 and 70°C [17]. Cadmium (Cd) removal rate increased with temperature increasing [17]. It is correlated with our investigations: rate of aluminium anodes dissolving ($Al \rightarrow \{electrolysis\} Al^{3+}$) increases with temperature increasing [10-14], so quantity of coagulant $Al(OH)_3$ also increases with temperature increasing, and, as result, the cadmium removal rate increases with temperature increasing too.

It was investigated the effect of various parameters like much higher temperature (200–500 °C), applied voltage (1.5–3.0 V), and feed gas (CO_2/H_2O) composition of 1, 9.2, and 15.6 in hydrocarbon fuel formation by electrolysis in molten carbonate (Li_2CO_3–Na_2CO_3–K_2CO_3; 43.5:31.5:25 mol%) and hydroxide (LiOH–NaOH; 27:73 and KOH–NaOH; 50:50 mol%) salts in works [17-21]. Enhancing hydrogen production from steam electrolysis in molten hydroxides via selection of non-precious metal electrodes was also described in [22 - 23].

The corrosion resistance of the coated aluminium alloy in a 3.5 wt.% NaCl solution (pH 6.5–7.5) and the influence of different surface treatment processes on the corrosion resistance of different samples were studied by scanning electron microscope (SEM) and electrochemical workstation in [24]. For this reason, we have planned to investigate copper and aluminium electrochemical corrosion rate dependence on temperature and electric current density during electrolysis in concentrated sodium chloride solution in water during heating by electric current from 20ºC to 180ºC using mathematical modelling.

I. Model

Electric current heats electrolyte during electrolysis if electrolyte volume is very small. We can calculate initial heating coefficient (b>0):

$$b = \frac{UI}{c\rho_1 V}\left[\frac{K}{s}\right], \quad (1)$$

where V is the electrolyte (it is, commonly, concentrated NaCl solution in water) volume, c is the electrolyte specific heat capacity, ρ_1 is the electrolyte density, I is the electric current value, U is applied voltage between anode and cathode. Heat transfer coefficient to environment, a>0, is proportional to difference between the electrolyte temperature (in ºC), $T(t)$, and the environment temperature T_0. Appropriate differential equation is as follows:

$$\frac{dT(t)}{dt} = b - a \cdot (T(t) - T_0);\ \left.\frac{dT}{dt}\right|_{t=+\infty} = 0; T(t=+\infty) = T_2;\ T(t=t_{diss}) = T_1. \quad (2)$$

Copper and aluminium anodes dissolve into the electrolyte with different rates at different temperatures [10-14], so we should assume that there is some external heating source having capacity b after dissolving of the anodes at t_{diss} (at T_1). Equation (2) gives:

$$a = \frac{b}{T_2 - T_0}. \quad (3)$$

Integrating of equation (2) leads to:

$$T(t) = T_2 - (T_2 - T_1) \cdot exp\left(\frac{b \cdot (t_{diss} - t)}{T_2 - T_0}\right); \frac{T_2 - T_0}{T_2 - T_1} = e^{\frac{bt_{diss}}{T_2 - T_0}}. \quad (4)$$

We can see that temperature T_2 depends on the heating coefficient b and $T_2 > T_1$.

II. Method

The rate of cylindrical anode dissolving into electrolyte can be calculated using Faraday's law of electrolysis [9-14]:

$$\frac{dm}{dt} = \frac{MI}{zF};\ dm(t) = -\rho L\pi \cdot d(R^2(t)). \quad (5)$$

Here, m is anode mass dissolved into the electrolyte, t is a time of the experiment, M is molar mass, I is the direct electric current value, F is the Faraday constant ($F \approx 96{,}500$ Cmol^{-1}), z is a charge of ions, R is anode radius, L is anode length immersed into the electrolyte, ρ is the anode density. Integrating of equation (5) gives at constant temperature:

$$R_{cyl}(t) = \sqrt{R_0^2 - \frac{I(T)}{z(T)} k_{cyl} \cdot t}; k_{cyl} = \frac{M}{F\rho L\pi}; t_{diss} = \frac{z(T)}{I(T)} \frac{R_0^2}{k_{cyl}}. \quad (6)$$

Charge of the Al ions is constant (z=+3) while average charge of the Cu ions increases with a complexing agent such as Cl^- [7] from z=+1 at T_0=20°C to z=+1.5 at T=100°C [3, 4, 10, 13], and to z=+2 at T_1=180°C [2]. The direct electric current value increased from I=2.8 A at T_0=20°C to I=3.05 A at T=100°C (and, theoretically, to I=3.3 A at T=180°C) for the Cu anodes while the direct electric current value increased from I=3.1 A at T_0=20°C to I=3.15 A at T=100°C (and, theoretically, to I=3.2A at T=180°C) for the Al anodes [10]. An average charge of the Cu ions increases in two times while electric current value increases on 18%, so we can assume I_{Cu}=<I>=3.05 A. It is a multicriteria problem [25] but we can use only the first criteria or increasing of the Cu ions average charge from +1 to +2 since it has the highest weight coefficient. We have obtained:

$$R^2(t)|_{R_{0Cu}}^{R(t)} = -k_{cyl}^{Cu} I_{Cu} \int_0^t \frac{dt}{z_{Cu}(t)}; R^2(t)|_{R_{0Al}}^{R(t)} = -k_{cyl}^{Al} \int_0^t \frac{I_{Al}(t)dt}{z_{Al}}. \quad (7)$$

Average charge of the Cu ions value linearly depends on temperature:

$$z(T) = (T + 140)/160, \quad (8)$$

but non-linearly depends on time (t<t_{diss}):

$$z(t) = \frac{1}{160}\left(T_2 + 140 - (T_2 - T_1)e^{\frac{b(t_{diss}-t)}{T_2-T_0}}\right). \quad (9)$$

First equation (7) gives for the Cu anodes:

$$R(t) = \sqrt{R_0^2 - \frac{160 k_{cyl} I_{Cu}(T_2-T_0)}{b(140+T_2)}\left(ln\left(e^{\frac{bt}{T_2-T_0}} - \frac{T_2-T_1}{140+T_2}e^{\frac{bt_{diss}}{T_2-T_0}}\right) - ln\left(1 - \frac{T_2-T_1}{140+T_2}e^{\frac{bt_{diss}}{T_2-T_0}}\right)\right)}. \quad (10)$$

III. Experimental results

We have done an experiment to investigate rate of the electrolyte heating by electric current during 20 min in concentrated NaCl solution (5 mol/kg [4] or 23.1% [26]) in water (Fig. 1). Warm electrolyte layers went up from the bottom to the surface. Temperature near the bottom was about 20°C and temperature near the electrolyte surface was increasing from 20°C to 60°C during 20 min.

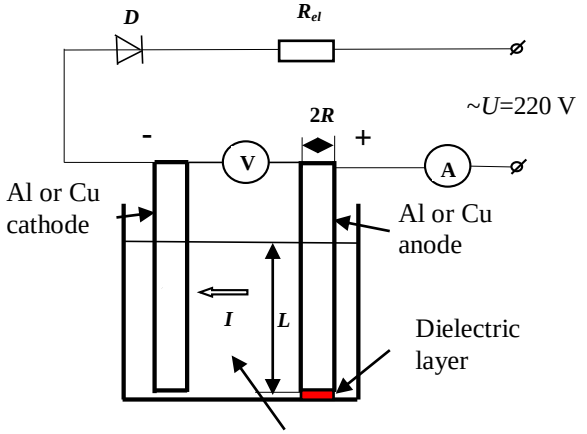

Fig. 1. Scheme of experimental equipment: ***D*** is a diode, R_{el} is an additional resistance (kettle), **A** is an ammeter, **V** is a voltmeter.

We have measured I=5.5 A; U=6 V; V=2·10^{-4}m^3, used literature data [26] ρ=1172 kg/m^3; c=3333 J/(kg·K), and calculated:

$$b = \frac{6V \cdot 5.5A}{3333J/(kg \cdot K) \cdot 1172kg/m^3 \cdot 2 \cdot 10^{-4}m^3} = 0.042K/s. \quad (11)$$

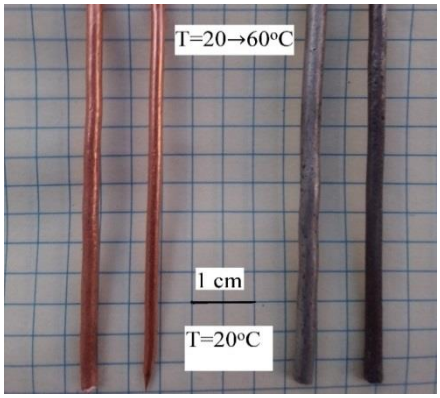

Fig. 2. Copper and aluminium anodes before and after electrolysis during 20 min in concentrated NaCl solution in water. Temperature distribution is non-uniform within the cylindrical anodes length.

Temperature distribution is non-uniform within the cylindrical anodes length, we can see that copper cylindrical anode dissolves and get cone shape with a top near the glass bottom where temperature is much smaller (Fig. 2). Such result shows that the rate of copper anode dissolving into the electrolyte decreases with temperature increasing as we have noted earlier [10-14]. On the other hand, we have also noted that the rate of aluminium anode dissolving into the electrolyte increases with temperature

increasing as we have noted earlier [10-14]. The electrolyte volume was more in 10 times earlier ($V = 2{\cdot}10^{-3}$ m^3) [10], so we have done experiments at constant temperatures.

We can analyse our published experimental results [10, 14]. We assume that temperature distribution is uniform within length of the cylindrical anode. We can find time of the copper anode dissolving at constant temperatures ($R_0 = 2.8$ mm; $L = 5$ cm):

IV. Analysis

4.1. Kinetics of the copper anode dissolving

$$t_{diss}(T = 20^oC, I = 2.8\ A) = \frac{R_0^2}{k_{Cu}} = \frac{2.8^2{\cdot}10^{-6}m^2}{1.25{\cdot}10^{-9}m^2/s} = 6{,}272s; \quad (12a)$$

$$t_{diss}(T = 100^oC, I = 3.05\ A) = \frac{R_0^2}{k_{Cu}} = \frac{2.8^2{\cdot}10^{-6}m^2}{1.154{\cdot}10^{-9}m^2/s} = 6{,}794s. \quad (12b)$$

Results (12a) and (12b) are experimental. Theoretical results are comparable (equation (6)):

$$k_{cyl}^{Cu} = \frac{M}{F\rho L\pi} = \frac{63.55{\cdot}10^{-3}kg/mol}{96{,}500C/mol{\cdot}8900kg/m^3{\cdot}\pi{\cdot}0.05m} = 4.71\cdot10^{-10}\frac{m^2}{A{\cdot}s}; \quad (13)$$

$$t_{diss}^{theor}(T = 20^oC) = \frac{z(T)}{I(T)}\frac{R_0^2}{k_{cyl}^{Cu}(T=20^oC)} = 5{,}945s; \quad (14a)$$

$$t_{diss}^{theor}(T = 100^oC) = \frac{1.5}{3.05A}\frac{R_0^2}{k_{cyl}^{Cu}(T=100^oC)} = 8{,}186s. \quad (14b)$$

We assume that T_1=180°C and get (0th iteration):

$$ln(\frac{T_2-T_0}{T_2-T_1})(T_2 - T_0) = bt_{diss}^{theor}(T = 20^oC) = 250K; \quad T_2^{(0)} = 280^oC. \quad (15)$$

Equation (10) gives:

$$R(t) = \sqrt{7.84 - \frac{5.473(T_2-T_0)}{140+T_2}(ln(\,e^{\frac{0.042t}{T_2-T_0}} - \frac{T_2-T_1}{140+T_2}e^{\frac{0.042t_{diss}}{T_2-T_0}}) - ln(\,1 - \frac{T_2-T_1}{140+T_2}e^{\frac{0.042t_{diss}}{T_2-T_0}}))}\ mm =$$
$$= \sqrt{7.84 - 3.388(ln(\,e^{0.000162t} - 0.623) + 0.975)}\ mm;\ t_{diss}^{theor(0)}(T = 20 \to 180^oC) = 9{,}200s. \quad (16)$$

1st iteration:

$$ln(\frac{T_2-T_0}{T_2-T_1})(T_2 - T_0) = bt_{diss}^{theor(0)}(T = 20 \to 180^oC) = 386K; \quad T_2^{(1)} = 202^oC. \quad (15a)$$

$$R(t) = \sqrt{7.84 - 3.04(ln(\,e^{0.00021t} - 0.56) + 0.83)}\ mm;\ t_{diss}^{theor(1)}(T = 20 \to 180^oC) = 8{,}770s. \quad (16a)$$

2nd iteration:

$$ln(\frac{T_2-T_0}{T_2-T_1})(T_2 - T_0) = bt_{diss}^{theor(1)}(T = 20 \to 180^oC) = 368K;\ T_2^{(2)} = 205^oC. \quad (15b)$$

$$R(t) = \sqrt{7.84 - 2.935(ln(\,e^{0.000227t} - 0.535) + 0.767)}mm;\ t_{diss}^{theor(2)}(T = 20 \to 180^oC) = 8{,}720s. \quad (16b)$$

3d iteration:

$$ln(\frac{T_2-T_0}{T_2-T_1})(T_2 - T_0) = bt_{diss}^{theor(2)}(T = 20 \to 180^oC) = 366K;\ T_2^{(3)} = 206^oC. \quad (15c)$$

$$R(t) = \sqrt{7.84 - 2.942(ln(\,e^{0.000226t} - 0.538) + 0.771)}\ mm;\ \ t_{diss}^{theor(3)}(T = 20 \to 180^oC) = 8{,}724s. \quad (16c)$$

We have calculated: T_2 = 206°C if heating coefficient is constant b = 0.042 K/s during electrolysis and after dissolving of the copper anode (Fig. 3).

Result (16c) allows us to calculate average dissolving coefficient of the copper cylindrical anode:

$$< k_{Cu} >= \frac{R_0^2}{t_{diss}^{theor(3)}} = \frac{2.8^2{\cdot}10^{-6}m^2}{8{,}724s} = 9\cdot10^{-10}m^2/s. \quad (17)$$

Such average coefficient is less than experimental

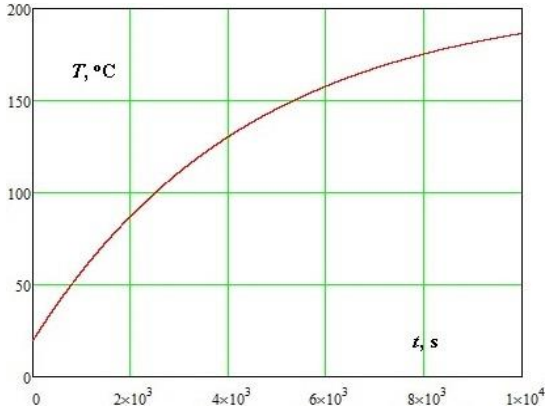

Fig.3. Temperature increasing during electrolysis with constant heating coefficient *b*=0.042 K/s.

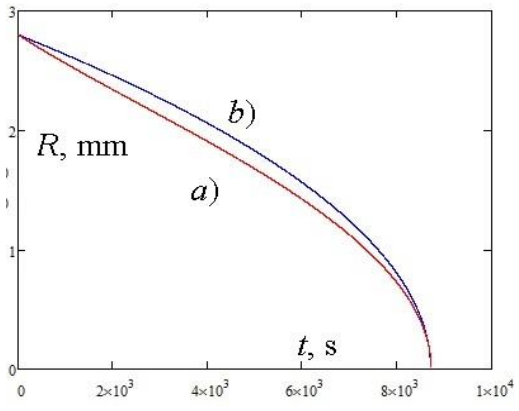

Fig.4. Kinetics of the copper anode dissolving: *a*) dissolving coefficient of the copper cylindrical anode is variable and depends on temperature; *b*) dissolving coefficient of the copper cylindrical anode is constant and does not depend on temperature.

coefficients ($1.25 \cdot 10^{-9}$ m^2/s at 20°C and $1.154 \cdot 10^{-9}$ m^2/s at 100°C). Increasing temperature leads to the anode dissolution rate value decreasing while electric current value increasing since average charge of the Cu ions increasing.

We can compare function (6) $R_{cyl}(t) = \sqrt{R_0^2 - < k_{Cu} > t}$ and function (16c) (Fig. 4).

The dissolving rate value, $\left|\frac{dR(t)}{dt}\right|$, decreases approximately in 4 times until $t \approx 6{,}700$ s ($T \approx 160$°C) due to the temperature-increasing-effect in case a) while the dissolving rate value increases all the time ($\frac{dR(t=t_{diss})}{dt} = -\infty$) due to the cylindrical-shape-effect in case b). Other mathematical methods without iterations were used for copper cylindrical anode degradation describing in [27, 30]. The methods give the same result, so we can conclude that they are correct. Similar methods were used for degradation rates calculations of Fe and Al anodes in [31].

4.2. Kinetics of the aluminium anode dissolving

We can analyse our published experimental results [10, 13]. We assume that temperature distribution is uniform within length of the cylindrical anode. We can find time of the aluminium anode dissolving at constant temperatures (R_0 = 2.8 mm; L = 4.5 cm):

$$t_{diss}(T = 20^oC, I = 3.1A) = \frac{R_0^2}{k_{Al}} = \frac{2.8^2 \cdot 10^{-6} m^2}{7.29 \cdot 10^{-10} m^2/s} = 10{,}754s; \quad (18a)$$

$$t_{diss}(T = 100^oC, I = 3.15A) = \frac{R_0^2}{k_{Al}} = \frac{2.8^2 \cdot 10^{-6} m^2}{8.42 \cdot 10^{-10} m^2/s} = 9{,}311s. \quad (18b)$$

Results (18a) and (18b) are experimental. Theoretical results are comparable (equation (6)):

$$k_{cyl}^{Al} = \frac{M}{F\rho L\pi} = \frac{27 \cdot 10^{-3} kg/mol}{96{,}500C/mol \cdot 2700 kg/m^3 \cdot \pi \cdot 0.045m} = 7.32 \cdot 10^{-10} \frac{m^2}{A \cdot s}; \quad (19)$$

$$t_{diss}^{theor}(T = 20^oC) = \frac{z}{I(T)} \frac{R_0^2}{k_{cyl}^{Al}(T=20^0C)} = 10{,}365s; \quad (20a)$$

$$t_{diss}^{theor}(T = 100^oC) = \frac{3}{3.15A} \frac{R_0^2}{k_{cyl}^{Al}(T=100^0C)} = 10{,}200s. \quad (20b)$$

We assume that the electric current value linearly depends on temperature:

$$I_{Al}(T) = (T + 4940)/1600, \quad (21)$$

but non-linearly depends on time ($t < t_{diss}$; T_2=206°C; T_0=20°C):

$$T(t) = 206 - 26e^{\frac{b(t_{diss}-t)}{186}}; \quad I_{Al}(t) = \frac{1}{1600}\left(5146 - 26e^{\frac{b(t_{diss}-t)}{T_2-T_0}}\right). \quad (22)$$

Second equation (7) gives for the Al anodes (0th iteration):

$$R(t) = \sqrt{R_0^2 - \frac{k_{cyl}^{Al}}{3}(3.216t - 72e^{\frac{bt_{diss}}{T_2-T_0}}(1 - e^{-\frac{bt}{T_2-T_0}}))}\{t_{diss}=10{,}754\ s\}=$$
$$= \sqrt{8.04 - 0.000785t - 0.2e^{-0.000226t}}\ mm;\ t_{diss}^{theor(0)} = 10{,}217s. \quad (23)$$

1st iteration:

$$R(t) = \sqrt{8.017 - 0.000785t - 0.177e^{-0.000226t}}\ mm;\ t_{diss}^{theor(1)} = 10{,}189s. \quad (23a)$$

2nd iteration gives the same result. Result (23a) allows us to calculate average dissolving coefficient of the aluminium cylindrical anode:

$$< k_{Al} >= \frac{R_0^2}{t_{diss}^{theor(1)}} = \frac{2.8^2 \cdot 10^{-6} m^2}{10{,}189s} = 7{,}7 \cdot 10^{-10} m^2/s. \quad (24)$$

Such average coefficient is greater than initial coefficient ($7.29 \cdot 10^{-10}$ m^2/s). Increasing temperature leads to the anode dissolution rate value increasing and electric current value increasing as we expected.

Treatment of landfill leachate wastewater by electrocoagulation process using an aluminium electrode was investigated in [28]. It was obtained that the optimum conditions of current density (X1) of 5.25 A/dm^2 = 525 A/m^2, inter-electrode distance (X2) of 1 cm and initial effluent pH of 7.83 lead to the maximum % colour removal, % total organic carbon (TOC) removal and minimum of power consumption. Such conditions should lead to enormous heating of the wastewater between the anode and cathode. Average temperature of the wastewater increased from 20 to 33ºC. The authors did not measure temperature of the wastewater between the electrodes.

4.3. Kinetics of spherical anode dissolving

Let us assume that the anodes have a spherical shape (Fig. 5).

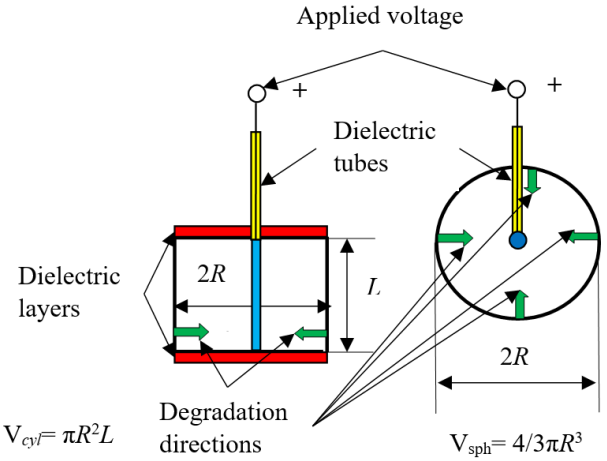

Fig. 5. Schemes of experiments. Cylindrical anode degrades to thin rod and spherical anode degrades to small ball.

We obtained in this case:

$$\frac{dm}{dt} = \frac{MI(T)}{z(T)F} = -\frac{4}{3}\rho\pi\frac{d(R^3(t))}{dt}; R(0) = R_0;$$

$$\frac{d(R^3(t))}{dt} = -\frac{3MI(T)}{4z(T)F\rho\pi}; R(0) = R_0; \quad k_{sph} = \frac{3MI(T)}{4z(T)F\rho\pi};$$

$$R^3(t)|_{R_{0Cu}}^{R(t)} = -k_{sph}^{Cu} I_{Cu} \int_0^t \frac{dt}{z_{Cu}(t)};$$
$$R^3(t)|_{R_{0Al}}^{R(t)} = -k_{sph}^{Al} \int_0^t \frac{I_{Al}(t)dt}{z_{Al}};$$

$$R_{sph}(t) = \sqrt[3]{R_0^3 - k_{sph}t}. \quad (25)$$

Dissolving time, t_{sph}, is calculated:

$$t_{sph} = \frac{R_0^3}{k_{sph}} = \frac{4R_0^3 z(T)F\rho\pi}{3MI(T)}. \quad (26)$$

We can compare (the spherical shape must be equal in volume to the rod shape):

$$\frac{t_{cyl}}{t_{sph}} = \frac{R_0^2 z(T)F\rho L\pi}{MI(T)} \frac{3MI(T)}{4R_0^3 z(T)F\rho\pi} = \{L = \frac{4}{3}R_0\} = 1,$$

so the dissolving time of spherical anode equals the dissolving time of cylindrical anode.

4.4. Amount of aluminium loss due to electrolysis per unit time calculation

Dependence of corrosion rate (CR), or weight-loss of aluminium per unit time, on temperature could be expressed in the form of the Arrhenius equation as [29]:

$$C_R^{Al}(T) = A_{Al}e^{-\frac{E_A^{Al}}{RT}} = k_{Al}(T)\pi L\rho_{Al}. \quad (27)$$

We can calculate the aluminium weight-loss per unit time using our experimental results [10, 14]:

$$C_R^{Al}(20^oC) = k_{Al}(20^oC)\pi L\rho_{Al} = 2.78 \cdot 10^{-7} kg \cdot s^{-1};$$

$$k_{Al}(T_1=20^oC) = 7.29 \cdot 10^{-10}\ m^2/s; \quad (28a)$$

$$C_R^{Al}(100^oC) = k_{Al}(100^oC)\pi L\rho_{Al} = 2.86 \cdot 10^{-7} kg \cdot s^{-1}$$

$$k_{Al}(T_2=100^oC) = 8.42 \cdot 10^{-10}\ m^2/s. \quad (28b)$$

Here, A_{Al} is the pre-exponential factor, E_A^{Al} is the activation energy of corrosion, R is the gas constant, T is

absolute temperature, k_{Al} [m^2/s] is the aluminium cylindrical anode radius-decreasing rate constant [10, 14], and L is anode length immersed into the electrolyte at temperature of the experiment (L(20ºC)=45 mm; L(100ºC)=40 mm). We can calculate the aluminium activation energy of corrosion and the pre-exponential factor using experimental results during electrolysis at room temperature and 100ºC:

$$E_A^{Al} = \frac{T_1 T_2 R}{T_2 - T_1} ln \frac{C_R(T_2)}{C_R(T_1)} = 322\, J \cdot mol^{-1} = 0.003\, eV;$$

$$A_{Al} = C_R(T) e^{\frac{E_A^{Al}}{RT}} = 3.17 \cdot 10^{-7}\, kg \cdot s^{-1} \qquad (29)$$

We can calculate the aluminium corrosion rate at temperature 180ºC during electrolysis into concentrated NaCl solution:

$$C_R^{Al}(180^oC) = 2.91 \cdot 10^{-7} kg \cdot s^{-1};\ k_{Al}(180^oC) = \frac{C_R^{Al}(180^o)}{\pi L \rho_{Al}} = 8.58 \cdot 10^{-10} m^2 \cdot s^{-1}. \qquad (28c)$$

Electric current value increases due to the Al^{3+} ions quantity increasing with temperature increasing, so we can propose such equation:

$$I^{Al}(T) = I_0^{Al} \cdot e^{-\frac{E_A^{Al}}{RT}};\ I_0^{Al} = 3.538\, A;\ I^{Al}(T) = 3.538 \cdot e^{-\frac{322\, J \cdot mol^{-1}}{RT}}. \qquad (30)$$

Eq. 30 gives:

$$I^{Al}(20^oC) = 3.1\, A;\ I^{Al}(100^oC) = 3.19\, A;\ I^{Al}(180^oC) = 3.25\, A. \qquad (31)$$

Measured values equal [10, 14]: $I_{exp}^{Al}(20^oC) = 3.1\, A;\ I_{exp}^{Al}(100^oC) = 3.15\, A$.

General quantity of the H^+ and Cl^- ions decreases during electrolysis at all temperatures since the H_2 and Cl_2 gases are formed near electrodes. We can calculate:

$$\Delta I = I_{theor}^{Al}(100^oC) - I_{exp}^{Al}(100^oC) = 0.04\, A;\ \frac{\Delta I}{I_{exp}^{Al}(100^oC)} = 0.013 = 1.3\%, \qquad (32)$$

so electric current value decreases on 1.3 %.

Conclusions

Increasing temperature leads to dissolution rate value of the copper anodes decreasing while electric current value increases since average charge of the Cu ions increases too. Such result can be called as "inverse Arrhenius law", so we can recommend to clear wastewater by electrocoagulation of Cu cathodes and anodes at lower temperature (20ºC).

Increasing temperature leads to dissolution rate value of the aluminium anodes increasing and electric current value increases too. Such result agrees with Arrhenius law, so we can recommend to clear wastewater by electrocoagulation of Al cathodes and anodes at higher temperature (100ºC).

The dissolving rate value of the copper anodes decreases approximately in 4 times due to the temperature increasing effect, while the dissolving rate value of the aluminium anodes increases all the time due to the cylindrical shape effect:

$$\frac{dR_{Al}^{cyl}}{dt} = \frac{-\langle k_{cyl} \rangle}{2\sqrt{R_0^2 - \langle k_{cyl} \rangle \cdot t}};\ t < t_{diss},$$

where t_{diss} is dissolving time of an anode.

Dissolving time of spherical anode equals dissolving time of cylindrical anode if spherical shape is equal in volume to the rod shape.

The spherical shape effect is less than the cylindrical shape effect until $t \approx 0.9 t_{diss}$, but enormously greater from $t \approx 0.9 t_{diss}$ to $t = t_{diss}$:

$$\frac{dR_{Al}^{sph}}{dt} = \frac{-R_0 \langle k_{cyl} \rangle}{3\sqrt[3]{(R_0^3 - R_0 \langle k_{cyl} \rangle \cdot t)^2}};\ t < t_{diss}.$$

Future investigations should include measuring of a wastewater temperature between electrodes during of EC processes.

General quantity of the H^+ and Cl^- ions decreases during electrolysis at all temperatures since the H_2 and Cl_2 gases are formed near electrodes. It decreases electric current value on 1.3 %.

Yarmolenko M.V. – Doctor of Philosophy in Physics and Mathematics, Associate Professor, Full Professor at Rauf Ablyazov East European University, Leading researcher of Scientific Research Institute of Armament and Military Equipment Testing and Certification;
Mogilei S.O. – Doctor of Philosophy in Technical Sciences, Associate Professor at Rauf Ablyazov East European University.

[1] T. Kizaki, M. O, and M. Kajihara, *Rate-Controlling Process of Compound Growth in Cu-Clad Al Wire during Isothermal Annealing at 483–543 K*. Materials Transactions, 61(1), 188 (2020); https://doi.org/10.2320/matertrans.MT-M2019207.

[2] C.S. Goh, W.L.E. Chong, T.K. Lee, and C.Breach, *Corrosion Study and Intermetallics Formation in Gold and Copper Wire Bonding in Microelectronics Packaging*. Crystals, 3(3), 391 (2013); https://doi.org/10.3390/cryst3030391.

[3] B. Beverskog and I. Puigdomenech (1998). *Pourbaix diagrams for the system copper-chlorine at 5–100 °C*. SKI Rapport 98:19; (1998). https://inis.iaea.org/collection/NCLCollectionStore/_Public/29/051/29051635.pdf.

[4] B. Beverskog and S.-O. Pettersson (2002). *Pourbaix Diagrams for Copper in 5 m Chloride Solution.* SKI Report 02, 23 (2020); https://www.stralsakerhetsmyndigheten.se/contentassets/4b1ef76c4151413998c76becb6da0570/0223-pourbaix-diagrams-for-copper-in-5-m-chloride-solution-pdf-320-kb

[5] T. Standish, J. Chen, R. Jacklin, P. Jakupi, S. Ramamurthy, D. Zagidulin, P. Keech, and D.Shoesmith, *Corrosion of copper-coated steel high level nuclear waste containers under permanent disposal conditions*, Electrochimica Acta, 211, 331 (2016); http://dx.doi.org/10.1016/j.electacta.2016.05.135.

[6] C. Lilja, F. King, I. Puigdomenech, Pastina B, *Speciation of copper in high chloride concentrations, in the context of corrosion of copper canisters*. Materials and Corrosion.; 72, 293 (2021); https://doi.org/10.1002/maco.202011778.

[7] P. Zhou and K.Ogle, *The corrosion of copper and copper alloys*. Encyclopedia of Interfacial Chemistry: Surface Science and Electrochemistry, 478 (2018);. https://doi.org/10.1016/B978-0-12-409547-2.13429-8.

[8] P. Zhou, M.J. Hutchison, J.R. Scully, and K. Ogle, *The anodic dissolution of copper alloys: Pure copper in synthetic tap water*. Electrochimica Acta, 191, 548 (2016); http://dx.doi.org/10.1016/j.electacta.2016.01.093.

[9] A.E. Broo, B.Berghult, T.Hedberg, *Copper corrosion in drinking water distribution systems — the influence of water quality*. Corrosion Science, 39 (6), 1119 (1997); https://doi.org/10.1016/S0010-938X(97)00026-7.

[10] M.V. Yarmolenko, *Copper, Iron, and Aluminium Electrochemical Corrosion Rate Dependence on Temperature*. In F. Zafar, A. Ghosal, & E. Sharmin (Eds.), Corrosion - Fundamentals and Protection Mechanisms, 35 (2022); IntechOpen. https://doi.org/10.5772/intechopen.100279.

[11] M.V. Yarmolenko, *Intrinsic Diffusivities Ratio Analysis in Double Multiphase Systems*. Defect and Diffusion Forum 413, 47 (2021); Trans Tech Publications, Ltd. https://doi.org/10.4028/www.scientific.net/ddf.413.47.

[12] M.V. Yarmolenko, *Intermetallics Disappearance Rate Analysis in Double Multiphase Systems*. Defect and Diffusion Forum, 407, 68 (2021); https://doi.org/10.4028/www.scientific.net/ddf.407.68.

[13] M.V. Yarmolenko, *Intrinsic Diffusivities Ratio Analysis in the Al-Cu System*. Physics and Chemistry of Solid State, 21(4), 720 (2020); https://doi.org/10.15330/pcss.21.4.720-726.

[14] M.V. Yarmolenko, *Copper and aluminium electric corrosion investigation and intermetallics disappearance in Cu-Al system analysis*. Physics and Chemistry of Solid State, 21(2), 294 (2020), https://doi.org/10.15330/pcss.21.2.294-299.

[15] M.V. Yarmolenko Diffusion Laws and Modified Pascal's Triangles. *Defect and Diffusion Forum*, 420, 3 (2022); https://doi.org/10.4028/p-k1ul2h.

[16] Amina Othmani, Abudukeremu Kadier, Raghuveer Singh, Chinenye Adaobi Igwegbe, Mohamed Bouzid, Md Osim Aquatar, Waheed Ahmad Khanday, Million Ebba Bote, Fouad Damiri, Ömür Gökkuş, Farooq Sher. *A comprehensive review on green perspectives of electrocoagulation integrated with advanced processes for effective pollutants removal from water environment*. Environmental Research, 215(1), 114294(2022); https://doi.org/10.1016/j.envres.2022.114294.

[17] Brahmi Khaled, Bouguerra Wided, Hamrouni Béchir, Elaloui Elimame, Loungou Mouna, Tlili Zied. *Investigation of electrocoagulation reactor design parameters effect on the removal of cadmium from synthetic and phosphate industrial wastewater*. Arabian Journal of Chemistry, 12(8): 1848 (2019); https://doi.org/10.1016/j.arabjc.2014.12.012.

[18] Ossama Al-Juboori, Farooq Sher, Abu Hazafa, Muhammad Kashif Khan, George Z. Chen, *The effect of variable operating parameters for hydrocarbon fuel formation from CO2 by molten salts electrolysis*, Journal of CO2 Utilization, 40, 101193 (2020); https://doi.org/10.1016/j.jcou.2020.101193.

[19] Farooq Sher, George Z. Chen. Electrochemical Production of Sustainable Hydrocarbon Fuels from CO2 Co-electrolysis in Eutectic Molten Melts. *ACS Sustainable Chemistry & Engineering*,8, 12877 (2020); https://doi.org/10.1021/acssuschemeng.0c03314.

[20] Nawar K. Al-Shara, Farooq Sher, Sania Z. Iqbal, Zaman Sajid, George Z. Chen. *Electrochemical study of different membrane materials for the fabrication of stable, reproducible and reusable reference electrode*. Journal of Energy Chemistry, 49, 33 (2020); https://doi.org/10.1016/j.jechem.2020.01.008.

[21] Mohd Hafiz Abu Hassan, Farooq Sher, Gul Zarren, Norhidayah Suleiman, Asif Ali Tahir, Colin E. Snape. *Kinetic and thermodynamic evaluation of effective combined promoters for CO2 hydrate formation*. Journal of Natural Gas Science and Engineering, 78, 103313 (2020); https://doi.org/10.1016/j.jngse.2020.103313.

[22] Farooq Sher, Nawar K. Al-Shara, Sania Z. Iqbal, Zaib Jahan, George Z. Chen. *Enhancing hydrogen production from steam electrolysis in molten hydroxides via selection of non-precious metal electrodes*. International Journal of Hydrogen Energy, 45(53), 28260 (2020); https://doi.org/10.1016/j.ijhydene.2020.07.183.

[23] Martin Khzouz, Evangelos I. Gkanas, Jia Shao, Farooq Sher, Dmytro Beherskyi, Ahmad El-Kharouf and Mansour Al Qubeissi. *Life Cycle Costing Analysis: Tools and Applications for Determining Hydrogen Production Cost for Fuel Cell Vehicle Technology*. Energies, 13(15), 3783 (2020). https://www.mdpi.com/1996-1073/13/15/3783.

[24] Fan L, Wang F, Wang Z, Hao X, Yang N, Ran D. *Study on the Influence of Surface Treatment Process on the Corrosion Resistance of Aluminium Alloy Profile Coating*. Materials. 16 (17), 6027 (2023); https://doi.org/10.3390/ma16176027.

[25] S. Mogilei, A. Honcharov, Y. Tryus, *Solving Multimodal Transport Problems Using Algebraic Approach*. In: Faure, E., Danchenko, O., Bondarenko, M., Tryus, Y., Bazilo, C., Zaspa, G. (eds) Information Technology for Education, Science, and Technics, ITEST 2022. *Lecture Notes on Data Engineering and Communications Technologies*, 178, 83 (2023) Springer, Cham; https://doi.org/10.1007/978-3-031-35467-0_6.

[26] O. M. Skarboviychuk, V. O. Ovcharuk, and V. G. Fedorov (2008). *Empirical functions of thermophysical characteristics of NaCl solutions as a function of temperature and concentration*. Food industry, 7, 111 (2008); http://dspace.nuft.edu.ua/jspui/bitstream/123456789/1320/3/7-36.pdf.

[27] M. Yarmolenko, S. Mogilei, *Iron, copper, and aluminium electrochemical corrosion in motionless and moving electrolytes investigation during electrolysis*, Results in Materials 20, 100479 (2023); https://doi.org/10.1016/j.rinma.2023.100479.

[28] P. Asaithambi, D. Beyene, A.R.A. Aziz, *et al. Removal of pollutants with determination of power consumption from landfill leachate wastewater using an electrocoagulation process: optimization using response surface methodology (RSM).* Appl Water Sci, 8, 69 (2018); https://doi.org/10.1007/s13201-018-0715-9.

[29] O. L. Olasunkanmi, Corrosion: Favoured, Yet Undesirable - Its Kinetics and Thermodynamics. Corrosion - Fundamentals and Protection Mechanisms: 15 (2022); https://doi.org/10.5772/intechopen.98545.

[30] M.V. Yarmolenko, *Rates of cylindrical and spherical copper anodes dissolving into concentrated NaCl water solution calculation during electrolysis and temperature increasing*, International Journal of Thermofluids 21, 100539 (2024); https://doi.org/10.1016/j.ijft.2023.100539.

[31] M.V. Yarmolenko, S.O. Mogilei, *Copper, Iron and Aluminium Electrochemical Corrosion Investigation during Electrolysis and Temperature Increasing*, Defect and Diffusion Forum 429: 93-106 (2023); https://doi.org/10.4028/p-5pUGB3.

М. В. Ярмоленко[1, 2], С. О. Могілей[1]

Дослідження електрохімічної корозії міді та алюмінію під час електролізу та нагрівання від 20ºC до 180ºC з допомогою математичного моделювання

[1]*Східноєвропейський університет імені Рауфа Аблязова, Черкаси, Україна, yarmolenko@suem.edu.ua*
[2]*Державний науково-дослідний інститут випробувань і сертифікації озброєння та військової техніки, Черкаси, Україна*

Наші дослідження показують, що електрохімічна корозія міді відбувається швидше, ніж електрохімічна корозія алюмінію при температурах, нижчих 180°C та густині електричного струму 3,000 A/m^2 (або 30 А/дм^2=3 мА/мм^2). Ми отримали: алюмінієві аноди (циліндричні або сферичні) розчиняються в концентрованому розчині NaCl під час електролізу швидше з підвищенням температури, а мідні аноди (циліндричні або сферичні) розчиняються повільніше з підвищенням температури від кімнатної до 180°C. Величина електричного струму також зростає з підвищенням температури. Дійсно, такий результат є неочікуваним. Загальна кількість йонів H^+ і Cl^- зменшується під час електролізу при всіх температурах, оскільки гази H_2 і Cl_2 утворюються поблизу електродів. Це зменшує величину електричного струму на 1.3%. Загальна кількість іонів Cu^+ і Cu^{2+} також зменшується з підвищенням температури. Ми припускаємо, що для збільшення значення електричного струму має бути тільки одна причина: середній заряд іонів міді збільшується від +1 при кімнатній температурі до +1,5 при 100°C і до +2 при 180°C, а заряд йонів алюмінію залишається незмінним +3. Для аналізу пропонується відповідна математична модель, а також використовуються літературні експериментальні дані.

Ключові слова: електрохімічна корозія, електроліз, електрокоагуляція, мідь, алюміній, математичне моделювання, металеві покриття.